Human Molecular Genetics, 2014, Vol. 23, No. 12 **3157–3165**
doi:10.1093/hmg/ddu026
Advance Access published on January 23, 2014

Thiol peroxidases ameliorate LRRK2 mutant-induced mitochondrial and dopaminergic neuronal degeneration in *Drosophila*

Dario C. Angeles[1], Patrick Ho[1], Ling Ling Chua[2], Cheng Wang[3], Yan Wann Yap[2], Cheehoe Ng[2], Zhi dong Zhou[2], Kah-Leong Lim[4], Zbigniew K. Wszolek[5], Hong Y. Wang[3] and Eng King Tan[1,2,3,*]

[1]Department of Neurology, Singapore General Hospital, Singapore, Singapore 169856 [2]National Neuroscience Institute, 11 Jalan Tan Tock Seng, Singapore, Singapore 308433 [3]Duke-NUS Graduate Medical School, 8 College Road, Singapore, Singapore 169857 [4]Department of Physiology, National University of Singapore, Singapore, Singapore 117599 [5]Department of Neurology, Mayo Clinic, Jacksonville, FL 32224, USA

Received September 15, 2013; Revised January 7, 2014; Accepted January 20, 2014

Mutations in leucine-rich repeat kinase 2 (LRRK2) are common causes of familial Parkinson's disease (PD). LRRK2 has been shown to bind peroxiredoxin-3 (PRDX3), the most important scavenger of hydrogen peroxide in the mitochondria, *in vitro*. Here, we examined the interactions of LRRK2 and PRDX3 in *Drosophila* models by crossing transgenic LRRK2 and PRDX3 flies. As proof of principle experiments, we subsequently challenged LRRK2 and LRRK2/PRDX3 flies with a peroxidase mimic, Ebselen. We demonstrated that co-expression of PRDX3 with the LRRK2 kinase mutant G2019S in bigenic *Drosophila* ameliorated the G2019S mutant-induced reduction in peroxidase capacity, loss of dopaminergic neurons, shortened lifespan and mitochondrial defects of flight muscles in monogenic flies expressing the G2019S alone. Challenges with Ebselen recapitulated similar rescue of these phenotypic features in mutant-expressing *Drosophila*. The peroxidase mimic preserved neuronal and mitochondrial and neuronal integrity and improved mobility and survival in mutant-expressing *Drosophila*. Taken together, our study provides the first *in vivo* evidence to suggest that phosphoinhibition of endogenous peroxidases could be a mechanism in LRRK2-induced oxidant-mediated neurotoxicity. Our therapeutic experiments also highlight the potential of thiol peroxidases as neuroprotective agents in PD patients carrying LRRK2 mutations.

INTRODUCTION

Parkinson's disease is characterized by progressive loss of dopaminergic (DA) neurons in the substantia nigra and deposition of Lewy bodies and neurites in surviving neurons (1–3). Important risk factors include age and mutations in disease-linked genes such as *LRRK2*, which 51 exons encoding a 278-kDa protein with multiple domains including a GTPAse and kinase region (2,4,5). A common LRRK2-G2019S mutation in the kinase domain that increases both kinase and apoptotic activities (6), is present in up to 40% in certain populations with ethnic-specific polymorphic risk and protective variants (7).

The cytotoxic role of oxidant-mediated damage has been recognized in the pathogenesis of familial Parkinson's disease (PD) (8). In fact, mutations in a number of PD-associated factors have been shown to increase vulnerability to oxidative stress (9). For example, mutation in Parkin T240R reduced its ubiquitin ligase function and ability to protect against oxidative stress while mutation in the kinase region of PTEN-induced putative kinase 1 inhibited its activity on HSP75 that compromised protection against oxidative stress (10,11). Recently, we have shown that mutant LRRK2 enhanced the phosphorylation of peroxiredoxin-3 (PRDX3) in cell cultures which resulted in the suppression of cellular peroxidase activity and exacerbated toxicity (12). This presents a possible mechanistic link between LRRK2-induced oxidative stress and neuronal death, although physiological implications of these interactions are unclear and *in vivo* evidence is lacking.

*To whom correspondence should be addressed at: Department of Neurology, Singapore General Hospital, Academia L4, 20 College Road, Singapore, Singapore 169856. Tel: +65 63214074; Fax: +65 63271137; Email: gnrtek@sgh.com.sg; ekl2ekl2@singnet.com.sg

Several classes of enzymes such as catalases and peroxidases that act on hydroperoxides have been conserved across species. These include the thiol-specific peroxidases that belong to the peroxiredoxin (Prx) and glutathione peroxidase (Gpx) families. Aside from their peroxidative functions, thiol peroxidases are involved in oxidative signaling and regulation of gene expression via redox transcription factors (13). Specifically, the potent H_2O_2 scavenger, Prxs, has been reported to play an important role in redox regulation (14). Significantly, Prxs are dysregulated in a number of medical diseases.

There are six mammalian Prx isotypes including the human mitochondrial PRDX3, which is a 2-cysteine thiol peroxidase (15). In *Drosophila*, the mitochondria contain Prxs, dPrx3 and dPrx5, which are crucial in maintaining redox homeostasis due to lack of ortholog for Gpx (16). Silencing of dPrxs resulted in deterioration of muscle and digestive tissues and decreased lifespan in flies. These effects were relieved by thioredoxin reductase but not by the mitochondrion-targeted catalase (17,18). Ebselen or 2-phenyl-1,2-benzisoselenazol-3 (2H)-one is a mimic of Gpx and Prxs (19). It reacts with hydroperoxide and peroxynitrite and has been shown as a lithium mimetic in mouse models of bipolar disorder (20). Early treatment with Ebselen has improved conditions in patients with acute ischemic stroke and bipolar disorder, suggestive of its neuroprotective properties (20,21).

In this study, we examined the potential protective effect of PRDX3 in an animal model and determined if a PRDX3 mimic could recapitulate similar effects. These questions have significant clinical implications as peroxidase mimics have been previously used in human disease trials (20,21).

RESULTS

LRRK2 inhibits PRDX3 in the fly brain

To examine LRRK2 and PRDX3 relations in *Drosophila*, we generated transgenic flies expressing human *LRRK2-WT-myc*, *LRRK2-G2019S-myc* or *PRDX3* fused with the upstream activation sequence (UAS) that binds the yeast *promoter-GAL4* transcription factor for tissue-specific expression. To examine interaction in the brain, neuronal expression of proteins was induced by crossing with the embryonic lethal abnormal vision (*elav*)-GAL4 driver line. Brain extracts were subjected to tag-based immunoprecipitation followed by the resolution of eluate proteins in gel. Immunoblots showed robust expression of wild-type (WT) LRRK2 in the LRRK2-WT line (referred as WT in the figure) and the bigenic line WT/PRDX3 while the kinase mutant variant of LRRK2 was expressed in the LRRK2-G2019S line (G2019S in the figure) and the bigenic line G2019S/PRDX3 (Fig. 1A). The LRRK2 protein was not expressed in the *UAS-LRRK2-WT*-encoding control line, which was not crossed with the GAL4 driver line. In the bigenic lines, LRRK2 proteins coprecipitated with PRDX3 in the brain extract (Fig. 1A). Image analysis also revealed the overlap of fluorescent signals from LRRK2 and PRDX3 staining (Fig. 1B) suggesting an interaction.

Next we detected the level of phosphorylated PRDX3 (p-PRDX3) among monogenic and bigenic flies. The extracts from G2019S/PRDX3 bigenic flies showed a marked increase in the level of p-PRDX3 compared with those of WT/PRDX3 bigenic flies and PRDX3 flies expressing PRDX3 alone (Fig. 1C) suggesting enhanced kinase activity of LRRK2-G2019S on PRDX3. To examine the effect of PRDX3 phosphorylation, we compared the peroxidase activities in the fly brain. We found a general decrease in peroxidase activity among LRRK2-expressing flies compared with PRDX3-expressing flies (Fig. 1D). Notably, the LRRK2-G2019S flies showed significant decrease in activity through age, most pronounced at 60 days post-eclosion (d.p.e.) (Fig. 1D). However, co-expression of PRDX3 in the G2019S/PRDX3 bigenic flies exhibited peroxidase activity that was not significantly lower than PRDX3 flies, suggesting that LRRK2-mediated phosphorylation of PRDX3 could lower functional peroxidase capacity.

To validate the decrease in peroxidase activity of LRRK2-G2019S flies, we compared the level of H_2O_2 in the fly brain. We found that LRRK2-expressing flies have significantly higher levels of peroxide compared with the non-expressing control and PRDX3-expressing flies (Fig. 1E). However, the peroxide level in bigenic G2019S/PRDX3 flies was significantly lower compared with LRRK2-G2019S flies (Fig. 1E), suggesting that LRRK2-mediated phosphorylation of PRDX3 could increase the peroxide load in brain tissues. In fact, the LRRK2 kinase mutant exhibited high level of proteins that had been modified by oxidants to complex with carbonyl groups (Fig. 1F). The levels of protein carbonyl were lower in bigenic G2019S/PRDX3 compared with LRRK2-G2019S flies. Together, these suggest that the LRRK2 mutant-mediated inhibition of peroxidase activity could elevate oxidant level and potentially oxidative stress.

PRDX3 ameliorates kinase mutant-induced loss of DA neurons

To examine the influence of G2019S-induced suppression of peroxidase function, we first compared the effect on longevity in monogenic and bigenic flies. Upon analysis, overall comparison showed a significant difference in survival curves at $P = 0.0043$ by log-rank test. Upon pairwise analysis, we found that neuronal expression of LRRK2 reduced the lifespan with only 52% of LRRK2-WT and 33% of LRRK-G2019S flies living to 60 d.p.e. (Fig. 2A). The lifespans of LRRK2-WT and LRRK-G2019S flies were significantly lower at $P = 0.03943$ and 0.03187, respectively, compared with driver control with a survival rate of 85.3% at 60 d.p.e. (Fig. 2A). The survival rate of G2019S flies was also lower than PRDX3 flies which exhibited 79% survival at 60 d.p.e. (Fig. 2A). At 44 d.p.e., the difference in survival between G2019-expressing and control flies was already significant at $P = 0.05284$, while that of WT-expressing flies was not significant at $P = 0.1466$. Interestingly, however, co-expression of PRDX3 in the bigenic flies extended the lifespan of WT/PRDX3 and G2019S/PRDX3 flies by 15 and 27%, respectively, suggesting attenuation of the lethal effects of LRRK2 by PRDX3.

To examine if neuronal integrity is also affected by G2019S, we compared the number of DA neurons (six-paired clusters in each brain hemisphere). The transgene expression was first induced by the *dopa decarboxylase* (*ddc*)-GAL4 driver line followed by neuronal staining with antibody against a rate-limiting enzyme of dopamine synthesis, tyrosine hydroxylase (TH) for counting. Our results show that clusterwise differences in

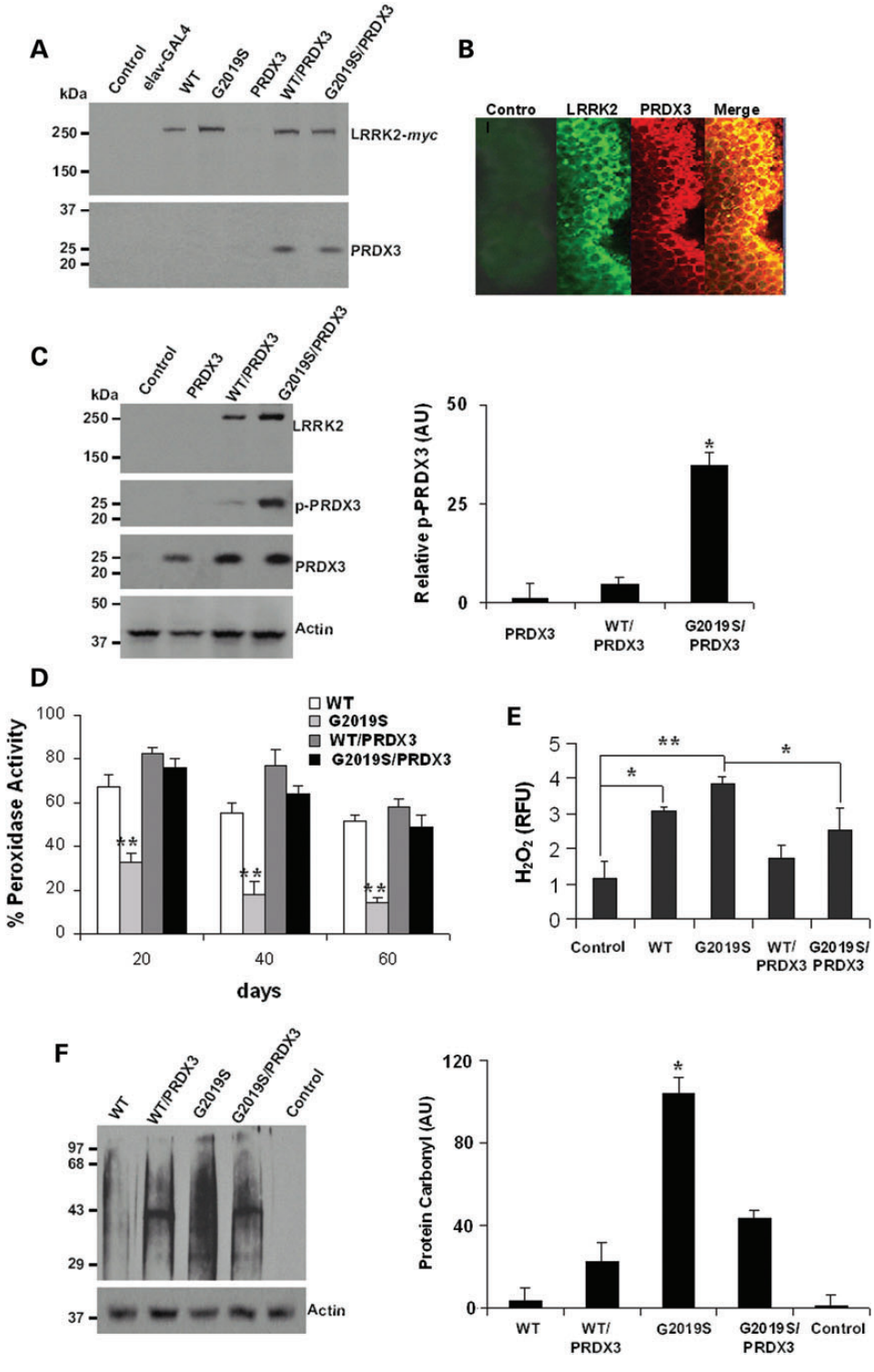

Figure 1. LRRK2 kinase mutant inhibits activity of PRDX3 in transgenic *Drosophila*. (**A**) Immunoblot of head lysates from 20 d.p.e. flies that were subjected to immunoprecipitation using *myc*-specific antibody. WT refers to the LRRK2-WT line, G2019S is the LRRK2-G2019S line and the control is *UAS-LRRK2* line that was not crossed with the driver. (**B**) Images showing colocalization of LRRK2 and PRDX3 signals in brain whole mounts. The control was probed with anti-LRRK2 as primary antibody. (**C**) Representative immunoblot showing p-PRDX3 detected by phospho-specific antibody. Chart showing relative p-PRDX3 levels over total PRDX3. *Significant increase from PRDX3 values at $P < 0.01$ by Student's *t*-test. AU, arbitrary unit. (**D**) Chart showing peroxidase activities as percent mean fluorescence ± SEM of values in PRDX3 lysate. Data were derived from three independent crosses that were background corrected and normalized to PRDX3 lysate values. **Significant decrease from PRDX3 values at $P < 0.01$ by Student's *t*-test. (**E**) Level of H_2O_2 as relative fulorescence unit ± SEM ($n = 4$) normalized to PRDX3 values. *,**Significant difference at $P < 0.05$ and $P < 0.01$ by one-way ANOVA with Bonferroni corrections. (**F**) Level of oxidized protein in LRRK2-variant-expressing flies relative to loading control. *Significant increase from all values at $P < 0.01$ by one-way ANOVA. Genotypes: *elav-GAL4*/+, *elav-GAL4-hLRRK2* variants, *elav-GAL4-PRDX3*, *elav-GAL4-hLRRK2; elav-GAL4-PRDX3.*

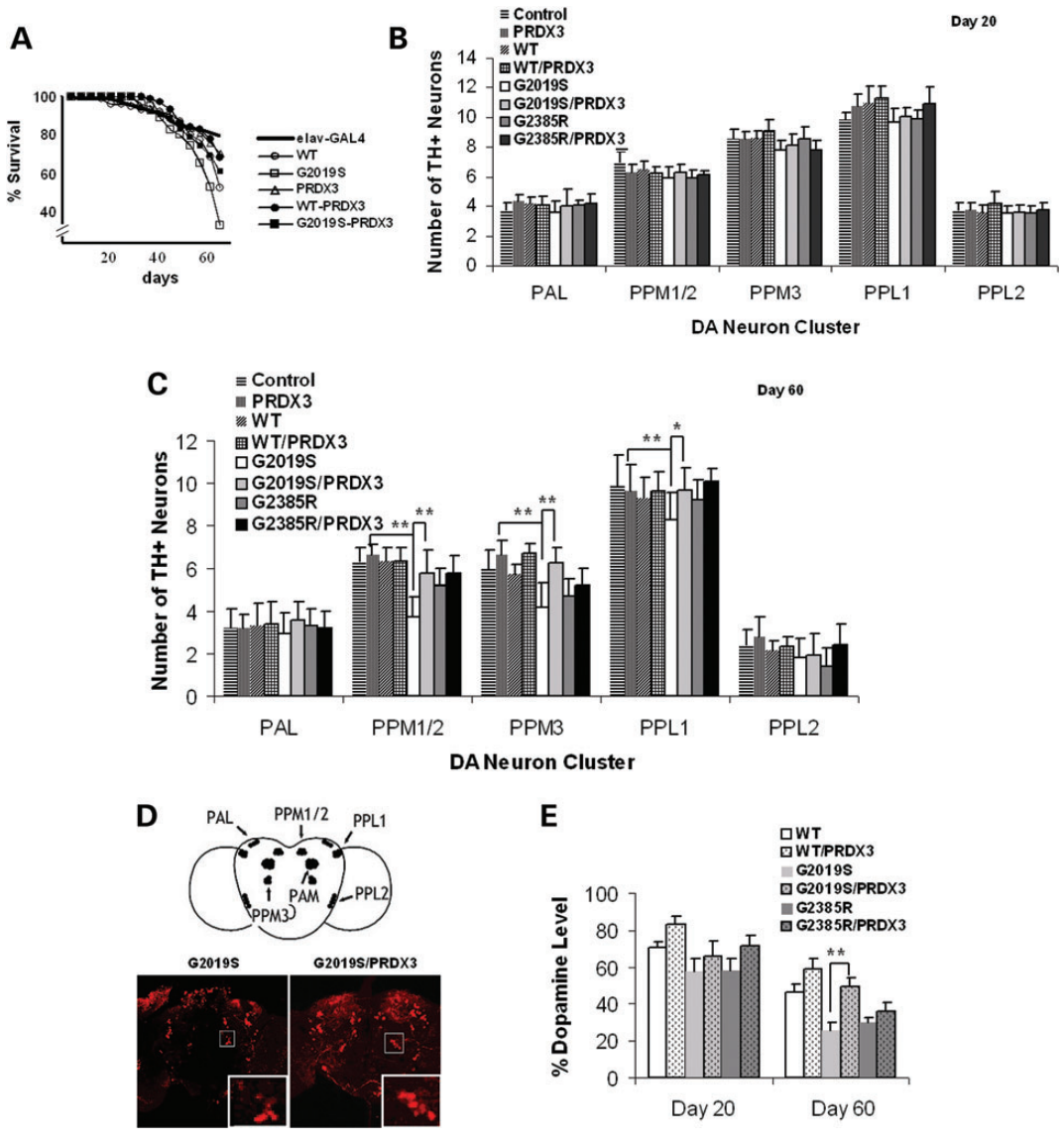

Figure 2. PRDX3 ameliorate mutant-induced DA neuronal degeneration. (**A**) Survival curves as percent living flies ($n = 3$, cohort of 50). Intergenotypic differences were analyzed by log-rank test, significant at $P < 0.05$. (**B**) Chart showing mean DA neuronal counts per cluster in the brain at 20 d.p.e. ($n = 3$; cohort of 20). (**C**) DA neuronal counts at 60 d.p.e. ($n = 3$; cohort of 20). *,**Significant difference at $P < 0.05$ and $P < 0.01$ by one-way ANOVA with Bonferroni corrections. The *elav*-GAL4 driver line was used as control. (**D**) Representative images of brain whole mount at 60 d.p.e. showing the PPM3 cluster (boxed) labeled with anti-TH antibody (red signal). Scale bar: 100 μm. (**E**) Dopamine level in fly brains as percent of mean absorbance ± SEM ($n = 4$) normalized to control. **Significant increase from counts in G2019S values at $P < 0.01$ by Student's *t*-test. PPL, protocerebral posterior lateral; PPM, protocerebral posterior medial; PAL, protocerebral anterior lateral. Genotypes: *ddc-GAL4/+*, *ddc-GAL4-hLRRK2*, *ddc-GAL4-hLRRK2; ddc-GAL4-PRDX3*.

neuronal number across genotypes were not significant at 20 d.p.e. (Fig. 2B). At 60 d.p.e., however, G2019S flies showed a significant 1.7-, 1.4- and 1.2-fold decrease in clusters PPM1/2, PPM3 and PPL1, respectively, compared with driver control (Fig. 2C). Although mutant LRRK2-G2385R flies, which express mutation in the WD40 domain at the C-terminus, showed slight reduction in the PPM3 cluster, the extent of neuronal loss seen in G2019S flies was not observed (Fig. 2C). In fact, the neuronal count in LRRK2-G2385 was consistently higher than in LRRK2-G2019S flies and was not significantly different from control, suggesting the non-toxic effect of G2385 mutation. These correlate with the observed reduction in kinase activity recent report on the decreased kinase activity in G2385 and C-terminally truncated forms of LRRK2 either on a WT or G2019S background (22). Since G2385R mutation was also observed to significantly increase LRRK2 binding to Hsp90 and decrease binding to 14-3-3 proteins, it is possible that G2385R mutation could affect LRRK2 binding to other protein partners including PRDX3.

When PRDX3 was co-expressed in bigenic G2019S/PRDX3 flies, we found that neuronal counts in the affected clusters were significantly increased compared with LRRK2-G2019S flies (Fig. 2C). In the PPM3 cluster, for example, the number of neurons was 1.5-fold higher in G2019S/PRDX3 compared with G2019S flies. The neuronal count in bigenic flies approximated those in PRDX3 or control flies. The preservation of

DA neurons in bigenic flies was consistent with intensified TH signal in immunostained brain sections (Fig 2D) and as higher levels of dopamine in bigenic than in kinase mutant fly brain at 60 d.p.e. (Fig. 2E). These show protection from the kinase mutant-induced loss of DA neurons by PRDX3.

PRDX3 and Ebselen ameliorate kinase mutant-induced motor dysfunction

Since neuronal loss has been linked to abnormalities in movement, we next compared the mobility in various genotypic lines. While there was a general reduction in climbing abilities at 40 d.p.e., G2019S flies showed marked decrease in climbing abilities compared with PRDX3 flies at 60 d.p.e. (Fig. 3A). However, climbing abilities of G2019S/PRDX3 flies were significantly higher than G2019S flies. As proof of principle experiment, we tested if the Prx mimic Ebselen could also protect from the effects of LRRK2. When sustained in Ebselen-supplemented medium, there was an ∼2.4-fold increase in the climbing abilities of G2019S flies which are comparable with those of bigenic flies (Fig. 3B). Conversely, parallel treatment with a thiol-containing reducing antioxidant thiourea did not prevent motor dysfunction in G2019S flies. These indicate improvement in motor abilities in the presence of Prxs.

To validate whether Ebselen-mediated improvement in mobility was related to the preservation of neurons. We did the clusterwise count of DA neurons and found that there was corresponding significant increase in the neuronal count in G2019S flies when fed with Ebselen. There was a general increase in clusters PPM1/2, PPM3 and PPL2 with the PPM3 or PPL1 counts increased by ∼28% (Fig. 3C). Therefore, the observed preservation of neurons reflected as improved climbing abilities, implicating thiol-dependent peroxidases in neuronal protection from LRRK2 kinase mutant-induced pathologies.

PRDX3 and Ebselen ameliorate kinase mutant-induced muscle and mitochondrial degeneration

To determine if LRRK2 mutant-induced impairment in mobility is related to changes in muscle morphology, we induced transgene expression in the thoracic flight muscles via the muscle-specific *24B*-GAL4 promoter in order to compare ultrastructure morphologies. In 40 d.p.e. non-transgenic control flies, myofibrils were tightly organized in parallel stripes, while those in age-matched kinase mutants were loosely disorganized with irregular banding patterns (Fig. 4A). However, muscle structures in Ebselen-fed kinase mutant flies showed similar morphologies as those seen in G2019S/PRDX3 bigenic flies (data not shown) and control flies (Fig. 4A).

Since muscles have high-energy demands, we next compared morphologies of the mitochondria. In G2019S flies, mitochondria were swollen, less dense with vacuolation and fragmented cristae (Fig. 4B). However, cristae in Ebselen-fed kinase mutants exhibited densely packed opaque structures, similar to those in control flies (Fig. 4B). Accordingly, we found that the proportion of deformed mitochondria in LRRK2-G2019S flies was ∼3- and

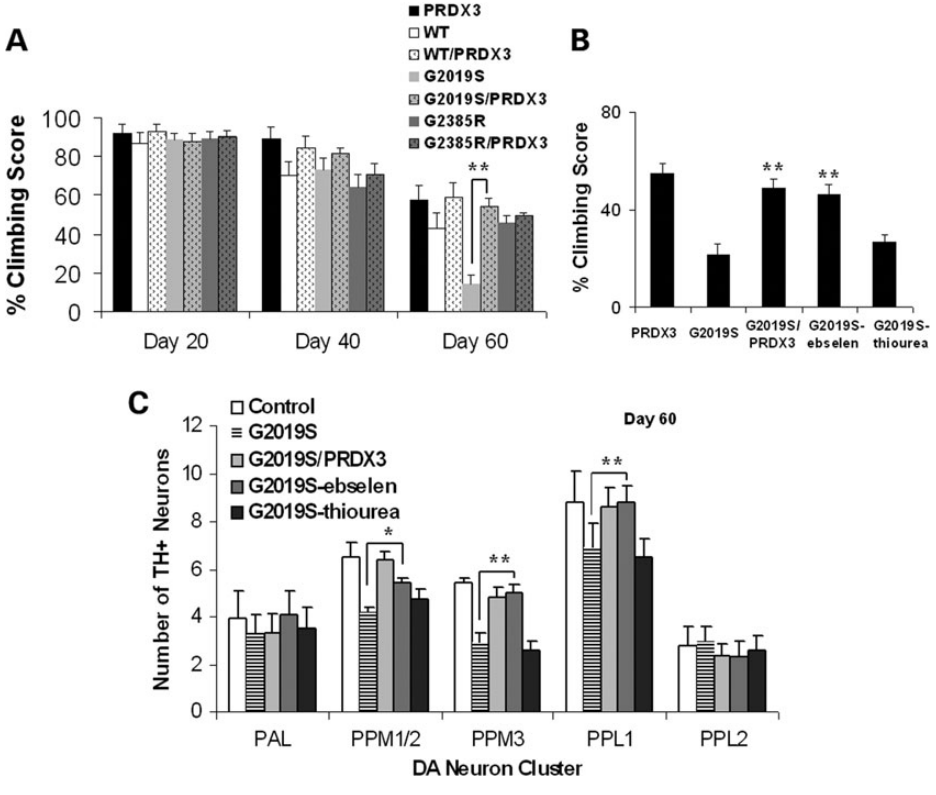

Figure 3 . PRDX3 and Ebselen ameliorate mutant-induced motor dysfunction. (**A**) Age-dependent climbing scores as percent of mean ± SEM ($n = 3$, cohort of 50) normalized to control. **Significant increase from G2019S values at $P < 0.01$ by one-way ANOVA with Bonferroni corrections. (**B**) Climbing scores as in (A). (**C**) DA neuronal counts by cluster ($n = 3$, cohort of 20). *,**Significant difference at $P < 0.05$ and $P < 0.01$ by one-way ANOVA with Bonferroni corrections.

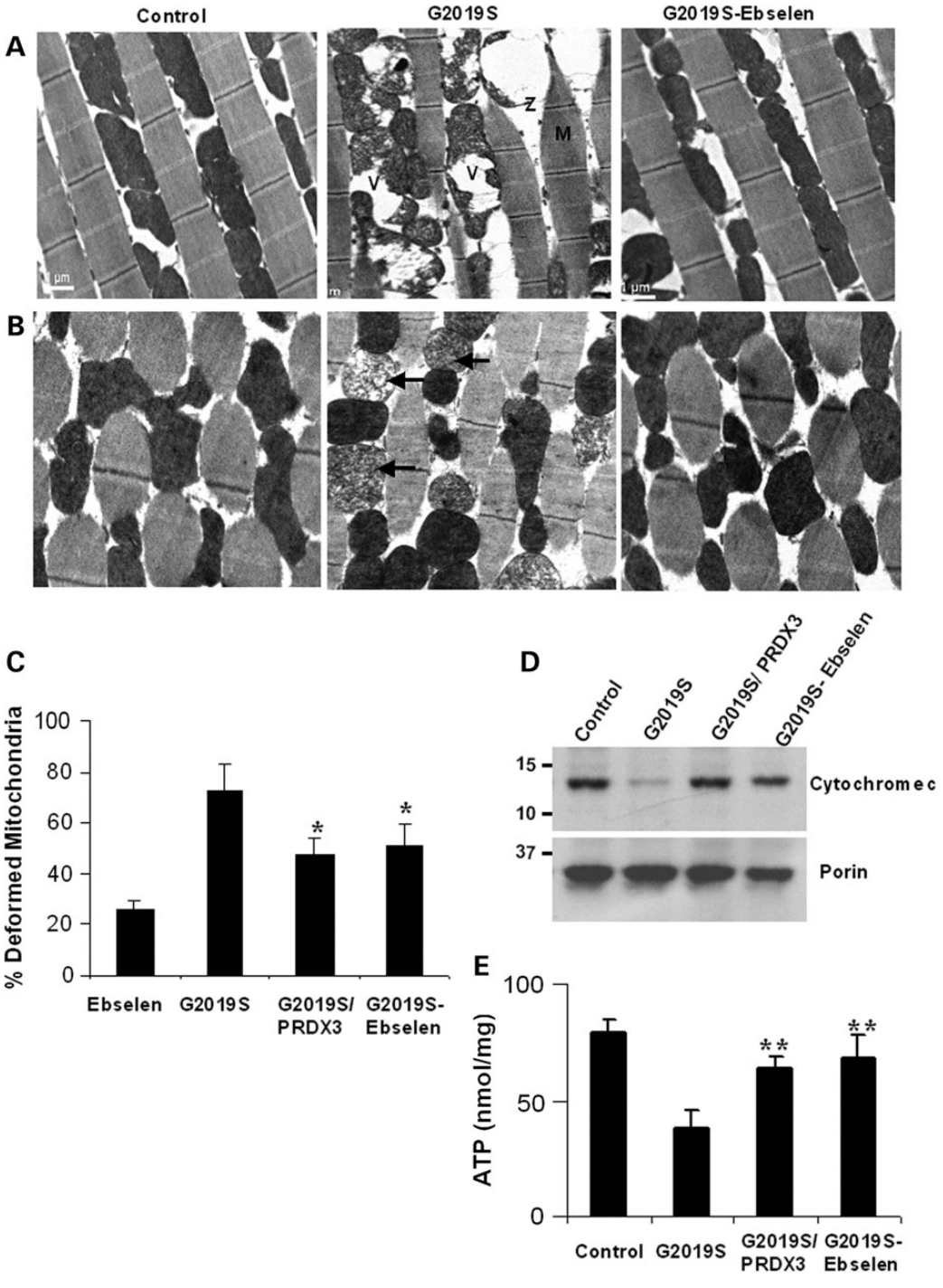

Figure 4 . PRDX3 and Ebselen ameliorate mutant-induced degeneration of muscle and mitochondria. (**A**) Transmission electron micrograph of longitudinal thoracic muscle sections showing the effects of Ebselen on kinase mutant-induced disruption of myofibrils with diffused Z-lines (Z) and M-bands (M). Swollen and vacuolated mitochondria (V) are also shown. (**B**) Transverse sections showing reduction in kinase mutant-induced fragmentation of cristae (arrows). Scale bars: 1 μm. (**C**) Chart showing percent of deformed mitochondria ± SEM normalized to driver control. Data were derived from the relative number of deformed over healthy mitochondria in 20 fields of five sections for each genotypic line. *Significant decrease from kinase mutant values at $P < 0.05$ by Student's *t*-test. (**D**) Immunoblot analysis of extracts for the level of cytochrome *c* in the mitochondria treated and untreated LRRK2-G2019S and driver control. (**E**) Comparison of ATP levels in the mitochondrial extracts showing mean ATP ± SEM ($n = 4$, cohort of 20 thoraces), corrected for blank and calculated from standard curve plot. **Significant increase from kinase mutant values at $P < 0.01$ by one-way ANOVA with Bonferroni corrections. Genotypes: *24B-GAL4/+*, *24B-GAL4-hLRRK2*, *24B-GAL4-hLRRK2; 24B-GAL4-PRDX3*.

4.6-fold higher than Ebselen-fed and control flies, respectively. However, deformed mitochondria in bigenic and Ebselen-fed kinase mutants were significantly lower than in kinase mutant flies at $P = 0.0281$ and 0.0442, respectively (Fig. 4C). These support the preservation of the mitochondrial morphologies in the presence of Ebselen and PRDX3 peroxidases.

To validate the observed conditions of the mitochondria, we compared the integrity of the mitochondrial membrane. In G2019S flies, the level of cytochrome *c* in the mitochondria is much lower compared with the control flies (Fig. 4D) indicating increased permeability of mitochondrial membrane in kinase mutant flies. However, the cytochrome *c* levels in bigenic and Ebselen-fed flies were markedly higher than in G2019S flies and near the levels found in the control. We further quantified the mitochondrial levels of adenosine triphosphate (ATP), which we found significantly lowered by ∼2.4-fold in LRRK2-G2019S flies, suggesting breach in mitochondrial integrity and function (Fig. 4E). However, the level of ATP was significantly higher in G2019S/PRDX3 flies and those fed with sustained doses of Ebselen than the levels in LRRK2-G2019S flies at $P = 0.0085$ and 0.0072, respectively. The ATP levels of G2019S/PRDX3 and Ebselen-fed G2019S flies were not different from levels found in the control. Together, these suggest Prx-mediated protection from potential compromise of the structure and function of the mitochondria induced by G2019S mutation in the kinase domain of LRRK2.

DISCUSSION

A number of disease-associated mutations in the kinase domain of LRRK2 have been shown to increase its kinase activity and exacerbate the degeneration of DA neurons (23,24). However, it remains unclear how such gain in function could lead to neuronal death. Incidentally, mutations in PD-linked genes including *LRRK2* have been shown to mediate increased vulnerability to oxidative stress (9,25). Moreover, oxidant-induced cell death has been observed in sporadic PD models exposed to environmental toxins (8). While enhanced kinase activity of mutant LRRK2 and oxidative damage are involved in the pathogenesis of PD, the unifying pathway linking these processes is not known.

Here, we showed that the expression of the LRRK2-G2019S kinase mutant resulted in neuronal death, increased oxidant load, deterioration of mitochondrial integrity and decreased respiratory function. These were concomitant with observed increase in the levels of p-PRDX3. Such LRRK2-PRDX3 interaction is not surprising as it is consistent with separate reports on their localization in the mitochondria (26,27). Moreover, the pathologies that we observed in kinase mutant flies were reminiscent of the consequential abnormalities in the mitochondria of oxidatively stressed flies (28). Based on these findings, it is possible that the LRRK2 phosphorylation site is proximal to the redox-active cysteine of PRDX3. The charged phosphate could pose a steric block preventing the oxidation of Cys^{47}-SH by H_2O_2 (29). Without sufficient antioxidant defense, the mitochondria, which conduct essential respiratory processes, becomes vulnerable to oxidative damage. Since these events were not evident in LRRK2-WT-expressing and control flies, we hypothesize that the enhanced phosphorylation and inhibition of the antioxidant function of PRDX3 induced by the kinase mutant, could be one mechanism involved in the oxidant-related death induced by LRRK2 kinase mutants.

Previously, the inhibition of Prx3 was shown to increase ROS-mediated damage of macromolecules, which induced the release of toxic by-products including aldehydes hydroxyl radical, lipid peroxide, aggregate, ubiquitinated protein and iron-catalyzed neurotransmitter catabolite (30–32). Furthermore, the intrinsic apoptotic pathway was triggered through the release of cytochrome *c* and activation of caspase-3 upon knockdown of Prx3 (12). Prx3 is also downregulated in the spinal motor neuron mitochondria of patients with motor neuron disease, while its phosphorylated form is increased in the midbrain of patients with PD (12,19). These support and highlight the importance of Prx3, such that its co-expression in bigenic flies in this study resulted in the amelioration of the lethal effects of the LRRK2 kinase mutant on flies.

To support the functional role of PRDX3, we further demonstrated that treatment with the Prx mimic, Ebselen, led to a reduction in H_2O_2, improved peroxidase function and viability of DA neurons and survival of flies. Ebselen-rescued LRRK2-induced pathologies, consistent with its dependence on the thioredoxin disulfide reductase system to catalyze the reduction of hydroperoxide and peroxynitrite (33). Ebselen has also been shown to upregulate expression of Prxs by inducing transcription of the antioxidant response element (19,34). Like PRDX3, Ebselen has mitochondrially directed anti-apoptotic effect via its action on membrane permeability transition (35,36). Unlike PRDX3, however, it has a selenium core that interacts with glutathione and other thiol compounds but without any binding site for substrate (37,38). While Ebselen has a peroxidase function, therefore, its actions are most likely varied and not specific.

Our findings suggest that further evaluation of Ebselen and other like compounds in LRRK2-linked PD is warranted. Ebselen is considered clinically safe but without proven use yet under the National Institutes of Health Clinical Collection. In a double-blind placebo controlled trial involving 302 acute ischemic stroke patients, significant improvement was noted in patients who started Ebselen within 24 h of stroke onset but not in those who started treatment after 24 h. Ebselen has also been shown to ameliorate neuronal toxicity in cell-culture model of superoxide dismutase 1-related familial motor neuron disease and 1-methyl-4-phenylpyridinium PD model (19,39). Considering these, it is not surprising that Ebselen recapitulated the activities of PRDX3.

In conclusion, we provided the first *in vivo* evidence that co-expression of PRDX3 in bigenic *Drosophila* ameliorated G2019S mutant-induced loss of DA neurons, shortened lifespan and mitochondrial defects in the flight muscles. Challenge with Ebselen led to similar rescue of these phenotypic features in *Drosophila*. Clinical trials of this class of drugs in PD patients would be useful to determine if their neuroprotective effects are specific for the LRRK2-linked disease.

MATERIALS AND METHODS

Drosophila stocks, preparation and immunodetection

Promoter lines containing *elav*-GAL4, *ddc*-GAL4 and *24B*-GAL4 were obtained from Bloomington Stock Center (Bloomington, IN, USA). The generation of human LRRK2 transgenic lines was described previously (40). *PRDX3* was amplified from a pCDNA3.1 construct and cloned directionally into *Xho*1–*EcoR*1 site of the pUAST vector. The sequence-verified constructs were microinjected into w118 embryos by BestGene (Chino Hills, CA, USA). Flies were routinely raised at 25°C

on cornmeal media that were replaced every 3 days. The lifespan was assessed by monitoring survival of 50 flies in five cohorts for each genotype. Fly head homogenates were prepared and immunoaffinity purified as described (12). A 50-μg lysate in RIPA buffer was precleared by centrifugation and complexed with 1 μg of antibody for 3 h at 4°C in rotator. Samples were incubated with BSA-blocked sepharose overnight. Equal amounts of eluate protein were resolved by SDS–PAGE and detected using rabbit LRRK2 (1 : 500; Novus Biologicals, Littleton, CO, USA)-, PRDX3 (1:2000; Sigma-Aldrich, St. Louis, MO, USA)- or rabbit p-PRDX3 (1:500; PickCell Laboratories, Amsterdam, Netherlands)-specific primary antibodies, whereas host-specific Alexa Fluor 488 (Invitrogen, Carlsbad, CA, USA) or Texas Red conjugates were used as secondary antibodies. The densitometric analysis of proteins was performed using the ImageJ software (NIH, MD, USA).

Peroxide, peroxidase, protein oxidation and dopamine assays

The levels of peroxide and peroxidase activity were measured according to the Amplex Red Kit protocol (Invitrogen). Briefly, reactions containing 50 μM reagent and 1 μg of fly head lysate in Na_2PO_4 buffer were incubated for 30 min at room temperature to measure peroxide level. The peroxidase activity was measured with the addition of 1 mM H_2O_2 per added. Fluorescence intensity was measured at Ex/Em 530 nm/590 nm. To quantify protein oxidation, 5 μg of brain extract was derivatized to 2,4-dinitrophenylhydrazone (DNP-hydrazone) by reaction with 2,4-dinitrophenylhydrazine. The protein carbonyl was detected by immunoblotting using anti-DNP moiety (1:150) (Millipore, Billerica, MA, USA). Dopamine was measured by HPLC with potentials set at $E_1 = -300$ mV, $E_2 = +200$ mV, $E_{GC} = +350$ mV and 50 nA range (Shimadzu, Japan). One hundred microliters of head lysate in 0.5 N perchloric acid were assayed at 0.5 ml/min flow rate for 10 min. Chromatograph peak for DA was detected at 6 min elution time. Dopamine was measured by HPLC with potentials set at E1 = −300 mV, E2 = +200 mV, EGC = +350 mV and 50 nA range.

Mitochondrial ATP assay

The crude mitochondrial fraction was isolated from fly extracts using sequential sedimentation as described (12). Total ATP levels in cohorts of three 5-day-old flies were measured for each genotype. Ten heads per cohort were dissected and homogenized in 200 μl of extraction buffer, snap-frozen then boiled for 3 mins. The samples were centrifuged and the supernatants were mixed with the luminescent reagent (Roche, Indianapolis, IN, USA). Signals were extrapolated using standards and values calculated relative to total protein concentration.

Behavioral assays

For longevity experiments, day-old flies were transferred to fresh media every 3 days. The triplicate cohorts of 50 flies per genotype were monitored for survival daily. For comparison between genotypes, pooled cohort scores were analyzed using the log-rank test with $P < 0.05$ considered significant. For the climbing assay, motor ability was assessed at 15 min interval using the negative geotaxis assay as described (41). Three cohorts of 20 female and age-matched control flies were anesthetized and placed in a vertical plastic column (length, 25 cm; diameter, 1.5 cm). After a 2 h recovery period, flies were tapped to the bottom and the percentage of flies that climb to or above the top column line in 1 min was calculated. Triplicate trials were performed in each experiment at 15 min interval.

Histochemistry and transmission electron microscopy

Immunostaining was performed on whole-mount adult fly brains as described (41,42). The dissected brains were probed with rabbit TH (1:200; Sigma)- or rat *elav* (1:50; Developmental Studies Hybridoma Bank, Iowa City, IA, USA)-specific primary antibodies. For the DA neuron count, the number of neurons in different clusters was scored under confocal microscopy. Six brain sections from cohorts of five flies per genotype were analyzed using the Nikon NS Element AR 3.2 software. For TEM, 20 d.p.e. adult thoraces were hemisected, fixed overnight at 4°C in 2% paraformaldehyde, 3% glutaraldehyde in 0.1 M phosphate buffer, pH 7.4. Tissues were postfixed in 2% osmium tetroxide for 1.5 h, dehydrated in ethanol–acetone series then embedded in araldite. Ultrathin sections were observed under Jeol Jem1010. Ultrathin sections were picked up onto copper slot grids, stained with uranyl acetate and lead citrate then observed under Jeol jem1010 (Peabody, MA, USA).

Conflict of Interest statement. None declared.

FUNDING

This work was supported by the National Medical Research Council, Singapore Millennium Foundation and Duke NUS Graduate Medical School. Z.K.W. is partially supported by the NIH/NINDS P50 NS072187.

REFERENCES

1. Zimprich, A., Biskup, S., Leitner, P., Lichtner, P., Farrer, M., Lincoln, S., Kachergus, J., Hulihan, M., Uitti, R.J., Calne, D.B. *et al.* (2004) Mutations in LRRK2 cause autosomal-dominant parkinsonism with pleomorphic pathology. *Neuron*, **44**, 601–607.
2. Hernandez, D.G., Paisán-Ruíz, C., McInerney-Leo, A., Jain, S., Meyer-Lindenberg, A., Evans, E.W., Berman, K.F., Johnson, J., Auburger, G., Schäffer, A.A. *et al.* (2005) Clinical and positron emission tomography of Parkinson's disease caused by LRRK2. *Ann. Neurol.*, **57**, 453–456.
3. Paisan-Ruiz, C., Jain, S., Evans, E.W., Gilks, W.P., Simon, J., van der Brug, M., Lopez de Munain, A., Aparicio, S., Gil, A.M., Khan, N. *et al.* (2004) Cloning of the gene containing mutations that cause PARK8-linked Parkinson's disease. *Neuron*, **44**, 595–600.
4. Kachergus, J., Mata, I.F., Hulihan, M., Taylor, J.P., Lincoln, S., Aasly, J., Gibson, J.M., Ross, O.A., Lynch, T., Wiley, J. *et al.* (2005) Identification of a novel LRRK2 mutation linked to autosomal dominant parkinsonism: evidence of a common founder across European populations. *Am. J. Hum. Genet.*, **76**, 672–680.
5. Di Fonzo, A., Tassorelli, C., De Mari, M., Chien, H.F., Ferreira, J., Rohe, C.F., Riboldazzi, G., Antonini, A., Albani, G., Mauro, A. *et al.* (2006) Comprehensive analysis of the LRRK2 gene in sixty families with Parkinson's disease. *Eur. J. Hum. Genet.*, **14**, 322–331.
6. West, A.B., Moore, D.J., Choi, C., Andrabi, S.A., Li, X., Dikeman, D., Biskup, S., Zhang, Z., Lim, K.L., Dawson, V.L. and Dawson, T.M. (2007) Parkinson's disease-associated mutations in LRRK2 link enhanced GTP-binding and kinase activities to neuronal toxicity. *Hum. Mol. Genet.*, **16**, 223–232.

7. Tan, E.-K., Peng, R., Teo, Y.-Y., Tan, C.L., Angeles, D., Ho, P., Chen, M.-L., Lin, C.-H., Mao, X.-Y., Chang, X.-L. *et al.* (2010) Multiple LRRK2 variants modulate risk of Parkinson disease: a Chinese multicenter study. *Hum. Mutat.*, **31**, 561–568.
8. Dauer, W. and Przedborski, S. (2003) Parkinson's disease: mechanisms and models. *Neuron*, **39**, 889–909.
9. Imai, Y., Gehrke, S., Wang, H.Q., Takahashi, R., Hasegawa, K., Oota, E. and Lu, B. (2008) Phosphorylation of 4E-BP by LRRK2 affects the maintenance of dopaminergic neurons in Drosophila. *EMBO J.*, **27**, 2432–2443.
10. Jiang, H., Ren, Y., Zhao, J. and Feng, J. (2004) Parkin protects human dopaminergic neuroblastoma cells against dopamine-induced apoptosis. *Hum. Mol. Genet.*, **13**, 1745–1754.
11. Pridgeon, J.W., Olzmann, J.A., Chin, L.S. and Li, L. (2007) PINK1 protects against oxidative stress by phosphorylating mitochondrial chaperone TRAP1. *PLoS Biol.*, **5**, e172.
12. Angeles, D.C., Gan, B.-H., Onstead, L., Zhao, Y., Lim, K.-L., Dachsel, J., Melrose, H., Farrer, M., Wszolek, Z.K., Dickson, D.W. and Tan, E.-K. (2011) Mutations in LRRK2 increase phosphorylation of peroxiredoxin 3 exacerbating oxidative stress-induced neuronal death. *Hum. Mutat.*, **32**, 1390–1397.
13. Fomenko, D.E., Koc, A., Agisheva, N., Jacobsen, M., Kaya, A., Malinouski, M., Rutherford, J.C., Siu, K.L., Jin, D.Y., Winge, D.R. and Gladyshev, V.N. (2011) Thiol peroxidases mediate specific genome-wide regulation of gene expression in response to hydrogen peroxide. *Proc. Natl. Acad. Sci. USA*, **108**, 2729–2734.
14. Hanschmann, E.M., Godoy, J.R., Berndt, C., Hudemann, C. and Lillig, C.H. (2013) Thioredoxins, glutaredoxins, and peroxiredoxins – molecular mechanisms and health significance: from cofactors to antioxidants to redox signaling. *Antioxid. Redox. Signal.*, **19**, 1539–1605.
15. Fujii, J. and Ikeda, Y. (2002) Advances in our understanding of peroxiredoxin, a multifunctional, mammalian redox protein. *Redox Rep.*, **7**, 123–130.
16. Sohal, R.S., Arnold, L. and Orr, W.C. (1990) Effect of age on superoxide dismutase, catalase, glutathione reductase, inorganic peroxides, TBA-reactive material, GSH/GSSG, NADPH/NADP+ and NADH/NAD+ in Drosophila melanogaster. *Mech. Ageing Dev.*, **56**, 223–235.
17. Mockett, R.J., Sohal, B.H. and Sohal, R.S. (2010) Expression of multiple copies of mitochondrially targeted catalase or genomic Mn superoxide dismutase transgenes does not extend the life span of Drosophila melanogaster. *Free Radic. Biol. Med.*, **49**, 2028–2031.
18. Radyuk, S.N., Rebrin, I., Klichko, V.I., Sohal, B.H., Michalak, K., Benes, J., Sohal, R.S. and Orr, W.C. (2010) Mitochondrial peroxiredoxins are critical for the maintenance of redox state and the survival of adult Drosophila. *Free Radic. Biol. Med.*, **49**, 1892–1902.
19. Wood-Allum, C.A., Barber, S.C., Kirby, J., Heath, P., Holden, H., Mead, R., Higginbottom, A., Allen, S., Beaujeux, T., Alexson, S.E., Ince, P.G. and Shaw, P.J. (2006) Impairment of mitochondrial anti-oxidant defence in SOD1-related motor neuron injury and amelioration by Ebselen. *Brain*, **129**, 1693–1709.
20. Singh, N., Halliday, A.C., Thomas, J.M., Kuznetsova, O.V., Baldwin, R., Woon, E.C., Aley, P.K., Antoniadou, I., Sharp, T., Vasudevan, S.R. and Churchill, G.C. (2013) A safe lithium mimetic for bipolar disorder. *Nat. Commun.*, **4**, 1332.
21. Yamaguchi, T., Sano, K., Takakura, K., Saito, I., Shinohara, Y., Asano, T. and Yasuhara, H. (1998) Ebselen in acute ischemic stroke: a placebo-controlled, double-blind clinical trial. Ebselen Study Group. *Stroke*, **29**, 12–17.
22. Rudenko, I.N., Kaganovich, A., Hauser, D.N., Beylina, A., Chia, R., Ding, J., Maric, D., Jaffe, H. and Cookson, M.R. (2012) The G2385R variant of leucine-rich repeat kinase 2 associated with Parkinson's disease is a partial loss-of-function mutation. *Biochem. J.*, **446**, 99–111.
23. Gloeckner, C.J., Kinkl, N., Schumacher, A., Braun, R.J., O'Neill, E., Meitinger, T., Kolch, W., Prokisch, H. and Ueffing, M. (2006) The Parkinson disease causing LRRK2 mutation I2020T is associated with increased kinase activity. *Hum. Mol. Genet.*, **15**, 223–232.
24. West, A.B., Moore, D.J., Biskup, S., Bugayenko, A., Smith, W.W., Ross, C.A., Dawson, V.L. and Dawson, T.M. (2005) Parkinson's disease-associated mutations in leucine-rich repeat kinase 2 augment kinase activity. *Proc. Natl. Acad. Sci. USA*, **102**, 16842–16847.
25. Liou AK, L.R., Li, L. and Zigmond, M.J. (2008) Wild-type LRRK2 but not its mutant attenuates stress-induced cell death via ERK pathway. *Neurobiol. Dis.* **32**, 116–e124.
26. Rhee, S.G., Chae, C.H. and Kim, K. (2005) Peroxiredoxins: a historical overview and speculative preview of novel mechanisms and emerging concepts in cell signaling. *Free Radic. Biol. Med.*, **38**, 1543–1552.
27. Biskup, S., Moore, D.J., Celsi, F., Higashi, S., West, A.B., Andrabi, S.A., Kurkinen, K., Yu, S.W., Savitt, J.M., Waldvogel, H.J. *et al.* (2006) Localization of LRRK2 to membranous and vesicular structures in mammalian brain. *Ann. Neurol.*, **60**, 557–569.
28. Clark, I.E., Dodson, M.W., Jiang, C., Cao, J.H., Huh, J.R., Seol, J.H., Yoo, S.J., Hay, B.A. and Guo, M. (2006) Drosophila pink1 is required for mitochondrial function and interacts genetically with parkin. *Nature*, **441**, 1162–1166.
29. Ellis, H.R. and Poole, L.B. (1997) Roles for the two cysteine residues of AhpC in catalysis of peroxide reduction by alkyl hydroperoxide reductase from Salmonella typhimurium. *Biochemistry*, **36**, 13349–13356.
30. Nagatsu, T. and Sawada, M. (2006) Cellular and molecular mechanisms of Parkinson's disease: neurotoxins, causative genes, and inflammatory cytokines. *Cell Mol. Neurobiol.*, **26**, 781–802.
31. Spencer, J.P., Jenner, A., Aruoma, O.I., Evans, P.J., Kaur, H., Dexter, D.T., Jenner, P., Lees, A.J., Marsden, D.C. and Halliwell, B. (1994) Intense oxidative DNA damage promoted by L-dopa and its metabolites. Implications for neurodegenerative disease. *FEBS Lett.*, **353**, 246–250.
32. Tsuchiya, Y., Okuno, Y., Hishinuma, K., Ezaki, A., Okada, G., Yamaguchi, M., Chikuma, T. and Hojo, H. (2007) 4-Hydroxy-2-nonenal-modified glyceraldehyde-3-phosphate dehydrogenase is degraded by cathepsin G. *Free Radic. Biol. Med.*, **43**, 1604–1615.
33. Fang, J., Zhong, L., Zhao, R. and Holmgren, A. (2005) Ebselen: a thioredoxin reductase-dependent catalyst for alpha-tocopherol quinone reduction. *Toxicol. Appl. Pharmacol.*, **207**, 103–109.
34. Tamasi, V., Jeffries, J.M., Arteel, G.E. and Falkner, K.C. (2004) Ebselen augments its peroxidase activity by inducing nrf-2-dependent transcription. *Arch. Biochem. Biophys.*, **431**, 161–168.
35. Boireau, A., Dubedat, P., Bordier, F., Coimbra, M., Meunier, M., Imperato, A. and Moussaoui, S. (1999) Effects of Ebselen, a glutathione peroxidase mimic, in several models of mitochondrial dysfunction. *Ann. N. Y. Acad. Sci.*, **893**, 254–257.
36. Boireau, A., Marechal, P.M., Meunier, M., Dubedat, P. and Moussaoui, S. (2000) The anti-oxidant Ebselen antagonizes the release of the apoptogenic factor cytochrome c induced by Fe2+/citrate in rat liver mitochondria. *Neurosci. Lett.*, **289**, 95–98.
37. Sies, H. (1993) Ebselen, a selenoorganic compound as glutathione peroxidase mimic. *Free Radic. Biol. Med.*, **14**, 313–323.
38. Schewe, T. (1995) Molecular actions of ebselen – an antiinflammatory antioxidant. *Gen. Pharmacol.*, **26**, 1153–1169.
39. Moussaoui, S., Obinu, M.C., Daniel, N., Reibaud, M., Blanchard, V. and Imperato, A. (2000) The antioxidant ebselen prevents neurotoxicity and clinical symptoms in a primate model of Parkinson's disease. *Exp. Neurol.*, **166**, 235–245.
40. Ng, C.H., Mok, S.Z., Koh, C., Ouyang, X., Fivaz, M.L., Tan, E.K., Dawson, V.L., Dawson, T.M., Yu, F. and Lim, K.L. (2009) Parkin protects against LRRK2 G2019S mutant-induced dopaminergic neurodegeneration in Drosophila. *J. Neurosci.*, **29**, 11257–11262.
41. Wang, L., Xie, C., Greggio, E., Parisiadou, L., Shim, H., Sun, L., Chandran, J., Lin, X., Lai, C., Yang, W.J. *et al.* (2008) The chaperone activity of heat shock protein 90 is critical for maintaining the stability of leucine-rich repeat kinase 2. *J. Neurosci.*, **28**, 3384–3391.
42. Whitworth, A.J., Theodore, D.A., Greene, J.C., Benes, H., Wes, P.D. and Pallanck, L.J. (2005) Increased glutathione S-transferase activity rescues dopaminergic neuron loss in a Drosophila model of Parkinson's disease. *Proc. Natl. Acad. Sci. USA*, **102**, 8024–8029.